Aerospace Science and Technology 47 (2015) 425–433

Contents lists available at ScienceDirect

Aerospace Science and Technology

www.elsevier.com/locate/aescte

Low velocity impact and quasi-static in-plane loading on a graded honeycomb structure; experimental, analytical and numerical study

S.A. Galehdari, M. Kadkhodayan *, S. Hadidi-Moud

Department of Mechanical Engineering, Ferdowsi University of Mashhad, Mashhad, Iran

ARTICLE INFO

Article history:
Received 29 May 2015
Received in revised form 13 October 2015
Accepted 14 October 2015
Available online 19 October 2015

Keywords:
Graded honeycomb structure
In-plane impact load
Quasi-static
Plateau stress
Deformation mode

ABSTRACT

Through the increasing development of technology in different industries, and the integral requirement of energy absorption, light shock absorbers such as honeycomb structure under in-plane and out-of-plane loads have been in the center of attention. The purpose of this research is to analyze the behavior of graded honeycomb structure (GHS) under low-velocity impact and quasi-static loading. To begin with using the lower-bound theorem, an analytical equation for plateau stress is represented, taking power hardening model into consideration. To compare the acquired analytical equations, empirical tests are conducted on test specimens made of aluminum 6061-O, under previously mentioned loading. Uniaxial tensile tests on each row material are performed to collect data on material properties. The low-velocity and quasi-static tests are conducted with Drop-weight and Santam compression machines, respectively. The quasi-static test is conducted to study the strain rate effect on behavior of the structure. Two experimental tests are simulated in ABAQUS/CAE. Based on the conducted comparisons, the numerical and analytical results indicate a satisfactory agreement with experimental results. Given the performed comparison between experimental and numerical mode shapes, a "V" deformation mode is distinguished for test specimen.

1. Introduction

Owing to the rapid development in automotive, transportation and aeronautics engineering, analyzing the energy absorption capacity in structures has became an important field of research. During the last decade, various materials and structures with high specific absorbing energy such as graded honeycomb structure and thin vessel structures have been studied [1,25]. One of the main applications of the cellular materials is in structural protection, due to their superior energy absorption and impact resistance. The basic applications pertaining to these characteristics are packaging of fragile components, with electronic devices as a dominant case, and various protective products such as helmets and shielding. Another emerging application is using cellular structures as, the core material for metal sandwich panels, which are proved to have superior performance over the counterpart solid plates of equal mass under shock loading [6,16,21,32,33].

In the quasi-static regime, the crushing response of most metal cellular structures indicates a typical stress–strain curve, including three regimes: an elastic response followed by a plateau regime with almost constant stress and eventually a densification regime of sharply rising stress [13,20]. The most important characteristic of graded honeycomb structures is that by changing the geometrical parameters of the structure such as height, thickness, cell size and inner angles, different mechanical characteristics could be obtained [2]. Low velocity impact can be treated as a quasi-static event, the upper limit of which can vary from 1 to 10 $\mathrm{m\,s^{-1}}$ depending on the target stiffness, material properties, and the impactor mass and stiffness [30]. Cantwell and Morton [4] classified low velocity up to 10 $\mathrm{m\,s^{-1}}$ by considering test techniques including Charpy, Izod and instrumented falling weight impact testing. Liu and Malvern [17] suggested that the type of impact can be classified according to the damage incurred. Abrate [1] and Robinson and Davies [29] defined a low-velocity impact as being one in which the through-thickness stress wave does not play any significant role in the stress distribution, and suggested a model to determine the transition to high velocity. A cylindrical zone under the impactor is considered to undergo a uniform strain as the stress wave propagates through the plate, resulting a compressive strain $\varepsilon_c = \frac{V_i}{V_s}$, where V_i is the impact velocity and V_s is the speed of sound in the material. For compressive strains below 1%, the low velocity condition can be considered. The speed of sound in a material is $V_s = \sqrt{\frac{E}{\rho}}$, where E and ρ are modulus of elasticity and density of the material, respectively.

* Corresponding author.
E-mail address: kadkhoda@um.ac.ir (M. Kadkhodayan).

http://dx.doi.org/10.1016/j.ast.2015.10.010
1270-9638/

Nomenclature

GHS	Graded Honeycomb Structure
A	Cross section area of GHS perpendicular to loading direction
b	Depth of GHS cell
c	Cell horizontal wall length
d	Cell wall thickness
e	Specific absorbed energy
e_f	Elongation
K	Coefficient of strain-hardening relation
L	Height of GHS
l	Cell inclined wall length
W	Width of the GHS
m	GHS mass
m_c	Mass of each cell
M_p	Fully plastic moment
n	Strain-hardening index
u	Strain energy per unit mass
U	Strain energy
V	Volume of GHS
V_c	Volume of each cell
y	Distance from neutral axis
σ_u	Ultimate stress
σ_y	Yield stress
σ_p	Plateau stress
ρ^*	Density of honeycomb structure
ρ_s	Density of honeycomb structure material
ε	Bending strain
ε_c	Compressive strain
ε_d	Locking strain
ϕ	Cell wall angle
ψ	Inclined wall rotation

The main purpose of energy absorbers is reduction the effect of impact load by its distribution within a time period. The main characteristics of energy absorbing cellular structures are absorbing energy in an irreversible manner, reducing reactive load, undergoing repeatable deformation mode, being compact, being light in weight, and having higher specific energy absorption capacity, being inexpensive and the ease of installation. The common forms of cellular structures are (1) open cell structures in which cells are arranged in a two dimensional regular or irregular array, and (2) closed cell structures in which plates are inter-connected and formed three dimensionally, partially open or closed with regular or irregular shaped cells. Honeycomb structures, considered as one of the primary shock absorbers, are widely used in automotive, aeronautics and packing industries. Scientifically speaking, banana peel which is a Functionally Graded Material (FGM) is a type of energy absorber [22]. Moreover, the human and bird bones are natural shock absorbers. The cancellous structure of bone leads to the absorption of applied shock as well as the reduction of bearing stress in joints [24]. Extensive research has been conducted in understanding the in-plane and out-of-plane behaviors of honeycombs. Deqiang et al. [5] analyzed the behavior of this type of structure under impact loads using LS-Dyna software. Song et al. [31] used a finite element model where the values of plateau stress and strain energy were obtained to investigate the influence of cells shape, impact load, relative density and strain hardening on the deformation mode and plateau stress. The results indicated that the values of plateau stress and energy absorption increased with a raise in cells' irregularity. Zou et al. [36] analyzed the in-plane dynamic destruction of regular honeycomb structures using FEM, and compared the obtained plateau stresses by analytical and numerical methods to each other. They also studied different mechanisms of structure cells deformation, and represented the stress-velocity diagrams. Ajdari et al. [3] analyzed the dynamic destruction behavior and the value of energy absorption in regular, irregular and FG honeycomb structures. They studied different modes of deformation and the value of energy absorption in these structures by FEM. Papka and Kyriakides [26,27] studied the load–displacement response of hexagonal-cell aluminum honeycombs, as well as circular polycarbonate honeycombs under in-plane uniaxial loading. They observed various deformation patterns (modes), which were related to the particular ratio between the components of the applied displacements or forces. Galehdari et al. [8,9] have compared the time history of reaction force of two honeycomb structures, i.e. the graded and with the same thickness. In another article, they have studied the effect of power hardening model for the GHS material on the plateau stress. Moreover, an optimization method has been introduced to maximize the specific absorbed energy. Fan and Zou [7] have studied the functionally graded honeycomb structures with defects. In this paper, the patterns and locations of defects, as well as the density gradients which affected the in-plane dynamic crushing behavior of honeycombs were studied. Based on the numerical results, the energy-absorption curves for systems with positive and negative densities were symmetric about the homogeneous structures. As the compression proceeds, for the honeycombs with positive and negative density gradients, the trends of energy-absorptive abilities went into reverse. Gunes et al. [12] investigated the damage mechanism and deformation of honeycomb sandwich structures reinforced by functionally graded plates under ballistic impact effect by means of explicit dynamic analysis using ANSYS LS-DYNA. The effect of material composition of functionally graded facesheets on the ballistic performance of honeycomb sandwich structures was investigated and the penetration and perforation threshold energy values which were the most considerable parameters on ballistic performance and ballistic limit of the sandwich structures were determined. Ghalami-Choobar and Sadighi [10] have investigated the high velocity impact response of sandwich specimens with FML skins and polyurethane foam by experimental and numerical approaches. The 3D finite element code, LS-DYNA was used to model impact of cylindrical projectile with clamped boundary condition. The results show the facesheets have major contribution on energy absorption of the sandwich specimens. Moreover, increasing core density did not significantly change absorbing energy in comparison with the effects of other parameters.

Muhammad et al. [23,24] simulated the behavior of graded honeycomb structure under impact load and presented an analytical equation for dynamic plateau stress corresponding to high velocities. The results of analytical equation were compared to those of numerical solution. In addition, to reduce the layer thickness in direction of panel sandwich thickness, the material hardness was also decreased. In another study, they investigated the in-plane response of the graded structure under medium and high velocity impacts. Different critical energy absorbing characteristics, e.g. deformation modes, collapsing mechanism, crushing stress, locking strain and total energy absorbed have been discussed. In above mentioned studies, the ideal elastic-perfectly plastic material model has been used to derive the plateau stress and specific energy of structure. However, a relatively large difference has been noticed between numerical and analytical results [22]. Zhu [35] has studied the large deformation pure bending of a wide

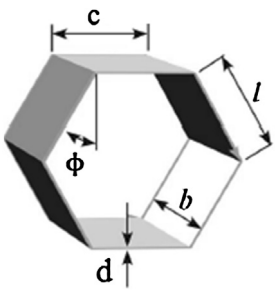

Fig. 1. Honeycomb structure cell.

plate made of a power-law-hardening material. In this research the bending moment of plastic hinge based on power hardening model has been derived for shells. In the current research, in order to reduce the difference, the plateau stress and specific energy of structure are derived based on power-hardening material model for the frame model. To verify the derived equation an FE analysis and an experimental test are conducted.

2. Mechanics of honeycomb structure

A typical honeycomb cell with its parameters is shown in Fig. 1.

Honeycomb structures transform in-plane kinetic energy into strain energy by crushing the rows which is equal to plastic hinge plastic energy. The most important parameters characterizing cellular material energy absorption properties are the plastic collapse stress generally known as the plateau stress and the relative density. The plateau stress has been determined using the upper and lower bound theorems. According to the upper bound theorem, an external load computed on the basis of an assumed mechanism, in which the forces are in equilibrium, is always greater than or equal to the true collapse load. On the other hand, the lower bound theorem states that an external load computed on the basis of an assumed distribution of internal forces, in which the forces are bounded by limit values and the forces are in equilibrium, is less than or equal to the true collapse load [11]. If a part of stress–strain diagram has a constant stress, it is called *plateau stress*. In fact, the value of plateau stress is not constant; however, its changes are negligible [18]. In deriving analytical equations, the value of σ_p is considered as constant. So far the elastic-perfectly plastic model has been used to derive the plateau stress. In this research, due to the previously high difference between the numerical and analytical results, the power hardening model is used. The stress distribution over the beam section for elastic perfectly plastic and strain hardening model is shown in Fig. 2. The plastic hinge moment of honeycomb wall is given by

$$M_p = 2b\int_0^{\frac{d}{2}} y\sigma\, dy \tag{1}$$

Based on the elastic-perfectly plastic model, Fig. 2b, the plastic hinge moment can be obtained as

$$M_p = \frac{b\sigma_y d^2}{4} \tag{2}$$

Based on Fig. 2a and considering the material model with the power hardening, by substituting $\sigma = K\varepsilon^n$ and $\varepsilon = \frac{2y}{d}\varepsilon_{\max}$ into Eq. (1) the corresponding plastic hinge moment can be obtained

$$M_u = \frac{b\sigma_u d^2}{2(n+2)} \tag{3}$$

where σ_u is the ultimate strength of the material of structure cell. Mangipudi et al. [19] have derived an equation for bending

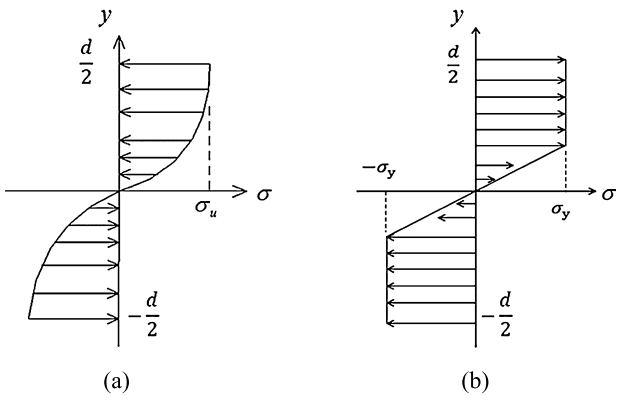

Fig. 2. Stress distribution for elastic perfectly plastic and strain hardening material models.

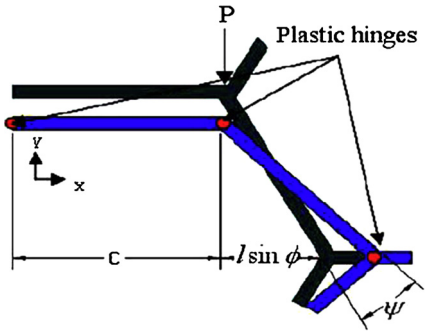

Fig. 3. Plastic collapse of inclined walls in the *Y* direction.

moment of a honeycomb cell wall based on Ludwik's hardening model. But any equation for plastic hinge moment has not been obtained. Based on upper and lower theorem and by using Eq. (2) the elastic-perfectly plastic plateau stress can be derived [11]

$$\sigma_p = \frac{\sigma_y d^2}{2(c + l\sin\phi)l\sin\phi} \tag{4}$$

The compressive load in the *Y* direction is transferred to the inclined walls and they bend like a frame. The plastic analysis shows that six plastic hinges [34] are required to define the complete 'collapse mechanism' of a cell. Fig. 3 shows the inclined wall undergoing angular rotation, ψ, with respect to its original position. An upper bound on the load acting on the wall is given by

$$P = \sigma_p(c + l\sin\phi)b \tag{5}$$

For $\frac{d}{l} < 0.25$, the axial and shear deflections are relatively small compared to bending deflections. Therefore, they do not have a noticeable influence on the plateau stress and bending moment [11]. Plastic hinge length is the length of plastic hinge region as shown in Fig. 4 for a honeycomb cell.

Plastic hinge length itself has a little effect on the load; however, it significantly changes the deformation geometry and the moment arm of the bending moment [28]. Hence, only the plastic hinge length effect is taken into account to derive the plateau stress equation.

The length of the plastic hinge is obtained by observing the values of bending moment, equivalent plastic strains and von Mises stress [15,14] at the integration points of the shell elements in the FE analysis and is equal to half of the cell wall thickness ($d/2$). The plastic hings are created in the both ends of the inclined wall and cannot resist the applied moment. Hence, the moment arm (l) is reduced to l–d. A lower bound on a collapse load is calculated

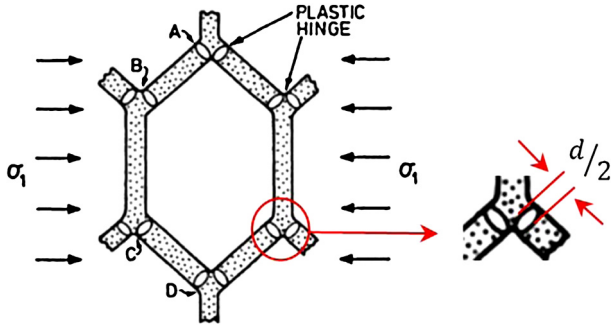

Fig. 4. Plastic hinge region in a honeycomb cell.

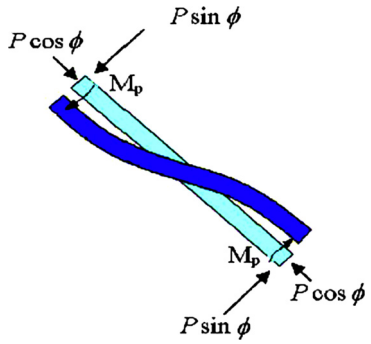

Fig. 5. Internal and external bending moments on the inclined wall.

by equating the internal negative moment on the cell wall to the external positive moment as shown in Fig. 5.

$$2M_p = P(l-d)\sin\phi \tag{6}$$

Substituting Eqs. (3) and (5) into Eq. (6), the power hardening model plateau stress is derived as

$$\sigma_p = \left(\frac{\sigma_u}{n+2}\right)\frac{d^2}{(c+l\sin\phi)(l-d)\sin\phi} \tag{7}$$

The corresponding locking strain can be calculated based on relative density (Eq. (8)).

$$\frac{\rho^*}{\rho_s} = \frac{(\frac{d}{l})(\frac{c}{l}+2)}{2(\sin(\phi)+\frac{c}{l})\cos(\phi)} \tag{8}$$

It is noteworthy that the relative density is the ratio of structure cell density to the density of the material of the honeycomb structure. In the above mentioned equation, ρ_s is the density of the material of honeycomb structure. The porosity, which in fact is the pore volume, is $1-\frac{\rho^*}{\rho_s}$. This value is approximately equal to the locking strain ε_d as [11]

$$\varepsilon_d = 1-\frac{\rho^*}{\rho_s} = 1-\frac{(\frac{d}{l})(\frac{c}{l}+2)}{2(\sin(\phi)+\frac{c}{l})\cos(\phi)} \tag{9}$$

It merits a mention that by increasing the thickness of honeycomb cell wall, the locking strain becomes lower than that of the calculated value in the equation mentioned above; however, the exact value could be obtained through the empirical tests. Parameter ε_d is the strain corresponding to the end of deformation in each row.

The force–displacement diagram of a honeycomb cell has three regions under compression. A linear-elastic regime is followed by a plateau of constant force, leading into a final regime of steeply rising force. Each regime is associated with a mechanism of deformation which can be identified by photographing method. On first loading, the cell walls bend. When a critical force is reached the cells begin to collapse; in materials with a plastic yield point it is by formation of plastic hinges at the section of maximum moment in the bent members. The critical force is approximately equal to constant (plateau) force. Eventually, at high deformations, the cells collapse sufficiently that opposing cell walls touch [11].

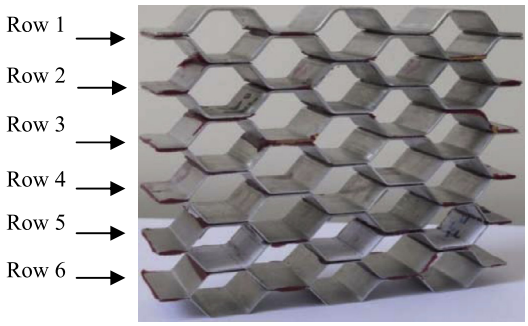

Fig. 6. Test sample of 6-row graded honeycomb structure.

3. Experiments

In order to validate the obtained analytical equations and defining the deformation mode, a quasi-static and low-velocity impact tests are carried out which are performed by Santam and Drop-weight machine, respectively. The experimental model is a 6061-O aluminum GHS. This structure has 6 rows with different thicknesses. Its rows are formed by ramrod and matrix and glued to each other by Adhesive-Film. The thickness of 1st to sixth rows is 1.6, 1.27, 1.016, 0.8125, 0.635 and 0.508 mm, respectively, Fig. 6. The geometrical dimensions are as $c = 15$ mm, $l = 12$ mm, $\phi = 36°$, $b = 28.5$ mm and $W = L = 13$ mm.

In order to obtain K and n of the power hardening stress–strain equation, uniaxial tensile test is performed on each thickness. The tensile test specimen is wire-cutted based on ASTM-A370 standard. The stress–strain diagrams of the uniaxial tensile tests on the standard specimens of AL-6061-O plate are obtained to determine the each row material properties. They are attained from the quasi-static tensile tests with the loading rate of 5 mm min^{-1}. The following equation is used to find the K and n for 0.508 mm thickness and the true stress–strain diagram is obtained, Figs. 7 and 8.

$$\ln\sigma = \ln K + n\ln\varepsilon \tag{10}$$

According to the mentioned procedure, material properties for each thickness of aluminum plates are found, see Table 1. The density and Poisson ratio of the used aluminum are taken as 2700 kg m^{-3} and 0.33, respectively. The obtained mechanical properties are used to define the material properties in finite element simulation.

According to Table 1, the experimental results show some discrepancy, thus for numerical simulation the average magnitude of material properties is used.

3.1. Quasi-static test

To study the behavior of GHS, a compression quasi-static test is performed on the test specimen with Santam machine. The loading rate is the same as the tensile test and the force–displacement diagram of compression test is obtained. The purpose of this test is to evaluate the effect of strain rate on the behavior of GHS. The loading condition of this test is shown in Fig. 9.

3.2. Low-velocity impact test

To study the behavior of GHS, a low velocity impact test is performed on two test specimens with Drop-weight machine, Fig. 10.

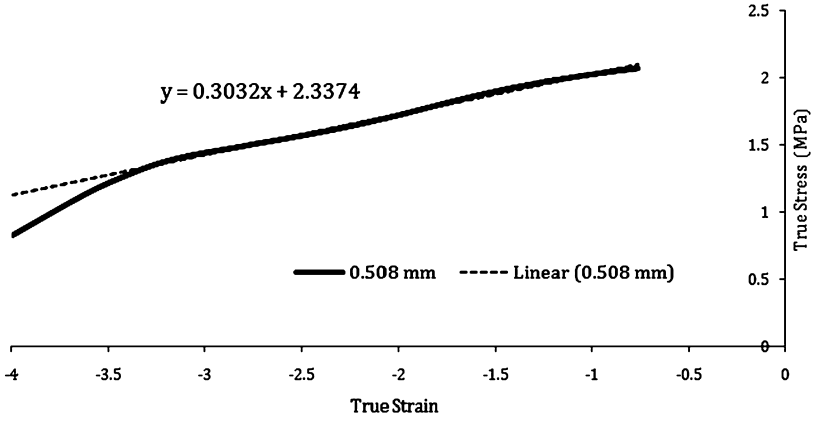

Fig. 7. True stress vs True strain diagram for 0.508 mm thickness plate.

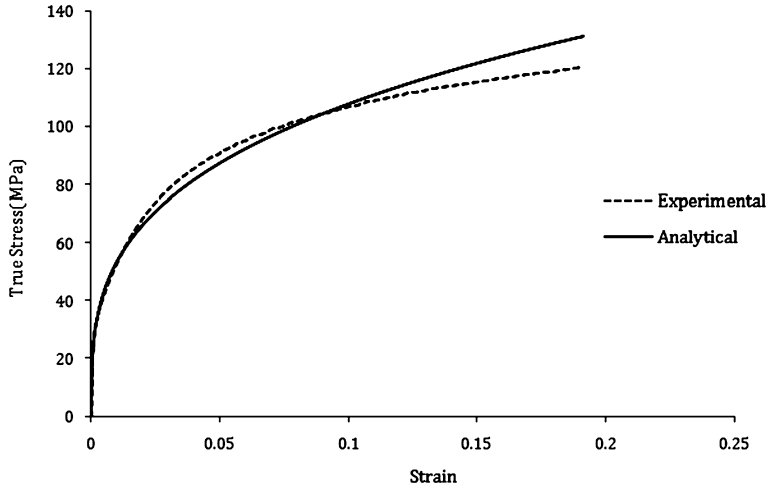

Fig. 8. Analytical and experimental true stresses vs true strains diagram for 0.508 mm thickness AL-6061-O plate.

Table 1
Mechanical properties of different thickness of AL-6061-O plate.

Thickness (mm)	E (GPa)	n	K (MPa)	e_f (%)	σ_u (MPa)	σ_y (MPa)
1.6	68.28	0.213	202.77	23.76	131.39	51.59
1.27	66.98	0.245	242.66	25.142	141	51.92
1.016	62.5	0.291	220.8	25.168	131	50.7
0.8125	63.51	0.229	205.6	30.72	141	50
0.635	64.3	0.247	228	27.06	134	48.15
0.508	66.81	0.303	217.27	31.092	124	53
Avg	65.39667	0.254667	219.5167	27.157	133.7317	50.89333

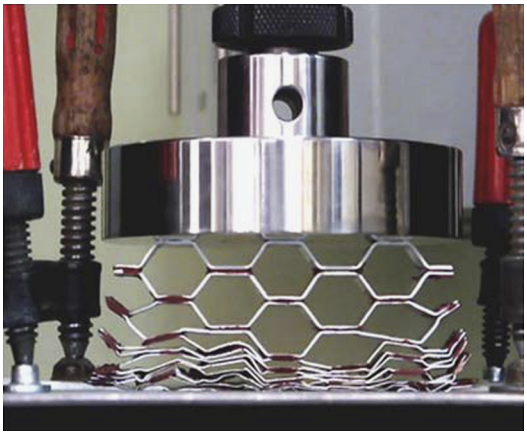

Fig. 9. Loading condition of quasi-static test.

Fig. 10. Drop-weight machine and the accelerometer.

In this test, 99 Joule kinetic energy is applied to the GHS by dropping a 9776.6 g steel block from a height of 120 cm. The acceleration of the dropped mass is measured by an accelerometer and then the reaction force base and deformation of the GHS are achieved. Based on these results, force–displacement diagram is attained. Due to friction and drag force of air, the kinetic energy and velocity decrease during of dropping. Therefore, the velocity of the

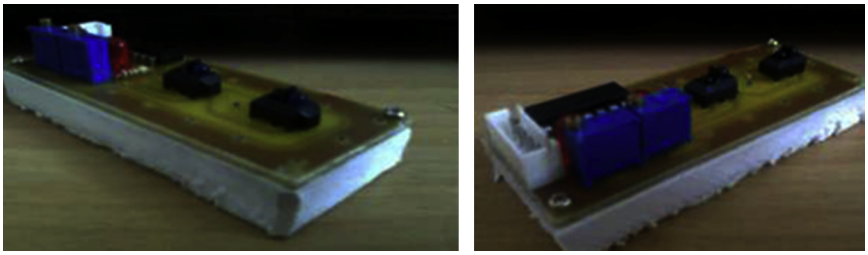

Fig. 11. Speedometer module.

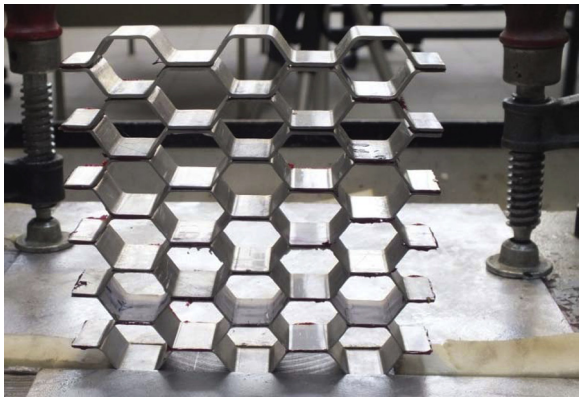

Fig. 12. Test specimen fixture.

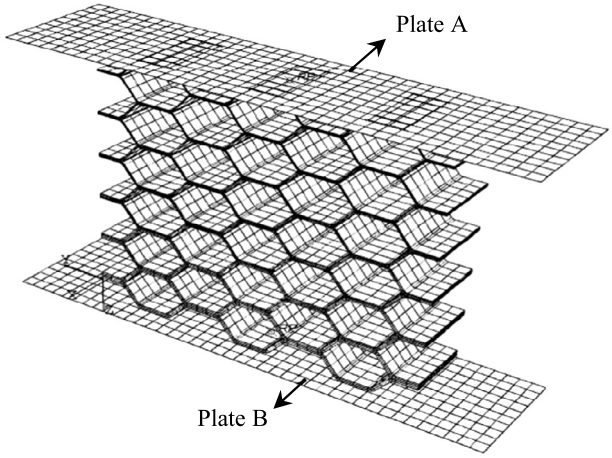

Fig. 13. FE model of GHS.

dropped mass is measured at the position the mass hits the test specimen using an infra-red speedometer, Fig. 11.

If there is not any loss of kinetic energy, the velocity can be calculated by $v = \sqrt{2gh} = \sqrt{2 \times 9.81 \times 1.2} = 4.85\ \mathrm{m\,s^{-1}}$, however, the measured velocity is 4.5 $\mathrm{m\,s^{-1}}$. A high-speed camera is used to record the deformation process of the structure. The fixture of test specimen is shown in Fig. 12. The test is performed on two specimens and using captured high speed film, the deformation mode of the GHS is distinguished.

4. Finite element analysis

The quasi-static and low-velocity impact test are also simulated in ABAQUS/CAE. The FE model made of aluminum 6061-O of graded honeycomb structure is demonstrated in Fig. 13. According to Table 1, the average magnitude of modulus of elasticity for this type of aluminium is 68.39 GPa and its density is 2700 $\mathrm{kg/m^3}$. Therefore, V_s is equal to 3250 and V_i is measured by speedometer as 4.5 m/s. The compressive strain on this type of aluminum is $\varepsilon_c = \frac{4.5}{5032.85} = 0.09\% < 1\%$, thus the strain rate is not considered. The dropped mass and the structure base are modeled by plates A and B, respectively. Hourglass controlled, 8 nodes, reduced integration linear brick elements (C3D8R) are used to mesh the structure and rigid bilinear quadrilateral elements (R3D4) are used to mesh plate A and plate B. For quasi-static and low velocity impact tests the final models have 3916 and 7688 elements, respectively. The boundary conditions are defined by constraining the discrete rigid plate, A, to move only in the Y plane and by fixing all the rotational and translational degrees of freedom of the discrete rigid plate, B. Interaction properties are imposed using a general contact condition and surface to surface kinematic contact conditions between the top element based surface of the structure and the rigid plate, A. A penalty contact condition with friction tangential behavior is applied between the bottom element based surface of the structure and the rigid plate, B. In this module based on test condition the coefficient of friction is considered equal to 0.6. The Adhesive-film between the rows is simulated by cohesive behavior using general contact interaction. For low velocity test the velocity of the plate A is assigned to its reference point using predefined field, and for quasi-static test the loading is applied on the structure by plate A. Using the measured material properties the plastic behavior of AL-6061O is defined using power hardening model for each row individually. The finite element problem is solved by dynamic/explicit solver for both loading conditions. The GHS material properties are represented in Table 1. In this simulation, the reaction force–deformation diagram of the structure obtained from numerical solution is compared to the analytical and experimental results.

5. Results and discussion

In analytical solution, the reaction force is calculated by multiplying the plateau stress by the cross section of each row and the structure deformation is also found by multiplying the locking strain by initial height of each row. According to the conducted numerical, analytical and experimental results, the reaction force–deformation diagrams of graded honeycomb structure under quasi-static loading are demonstrated in Fig. 14. Moreover, the obtained numerical and experimental deformed shapes of structure due to quasi-static loading are shown in Fig. 15.

According to Fig. 14, the numerical, experimental and analytical results retain an appropriate congruence. Moreover, the deformed shape of test sample obtained from experimental test has an acceptable similarity with the numerical deformed shape, Fig. 15. The reason for the difference between the analytical deformation and those of numerical and experimental results can be attributed to the usage of structure deformation equation, Eq. (9), as it was mentioned before. However, the obtained congruence of analytical and numerical results with experimental ones would be a robust support for the represented analytical and numerical simulation methods. Fig. 16 shows the force–time diagram of low-velocity test performed for two specimens. It shows that the results of both tests have a proper congruence.

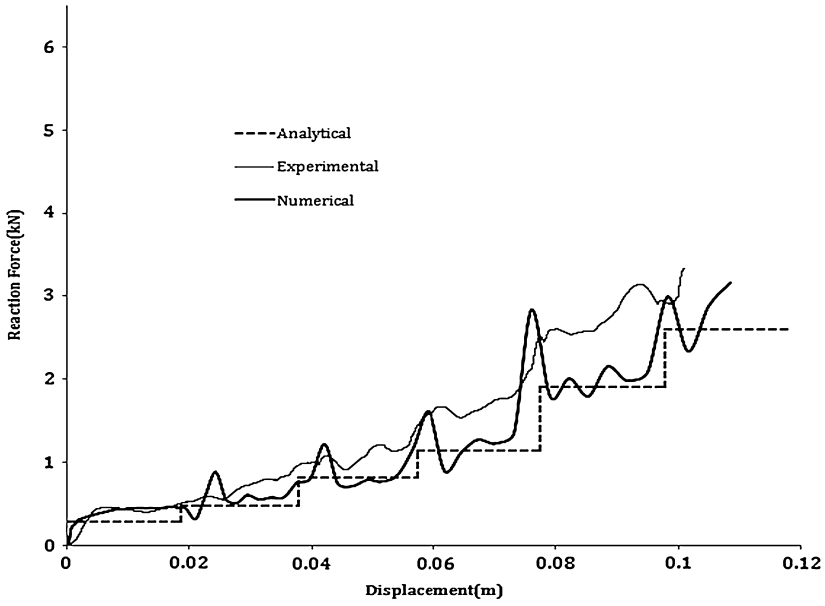

Fig. 14. Reaction force vs. displacement of the structure based on analytical, numerical and experimental results for quasi-static loading.

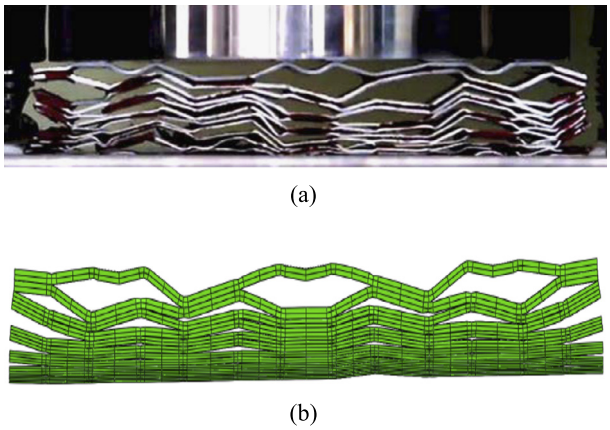

Fig. 15. Deformed shape of GHS under quasi-static loading; (a) experimental test, (b) numerical simulation.

Moreover, the analytical, numerical and experimental results of reaction force–deformation of graded honeycomb structure under low-velocity impact load are displayed in Fig. 17 and the results are of an appropriate accordance. Fig. 18 illustrates the obtained deformed shapes of numerical simulation and experimental tests. The deformed shape of test sample in experimental test is highly similar to that of numerical method.

Figs. 15 and 18 show the two different deformation mechanisms of quasi-static and low-velocity loading cases. In the former the deformation of each row (from bottom) starts before complete deformation of the last row. In the latter, however, the deformation in each row starts when the deformation is completed in the last row. The difference between two deformations mechanism is due to impact wave propagation in the structure. In low velocity loading, the sixth row experiences deformation when a compressive impact wave is propagated in the structure. Because of the clamped boundary condition at the bottom of structure, the compressive impact wave is reflected with double amplitude and deforms the row again. There is not any impact wave in quasi-

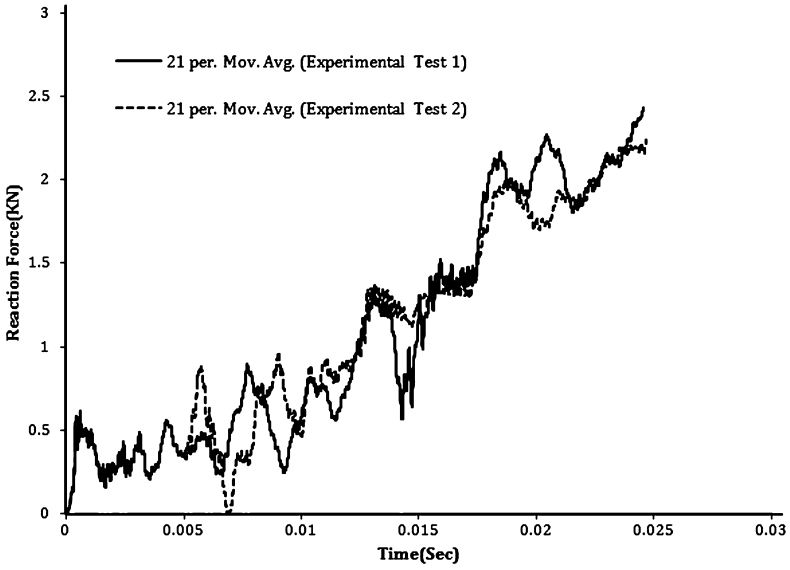

Fig. 16. Force vs. time diagram of two low-velocity tests.

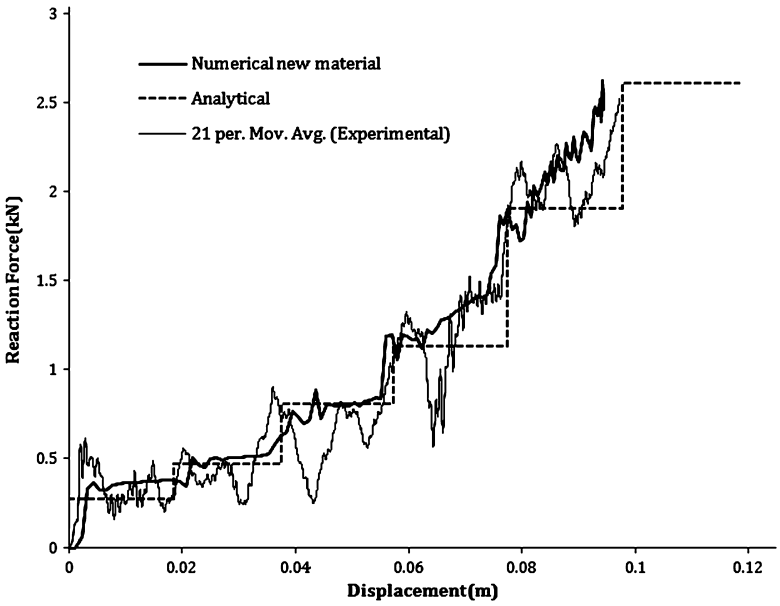

Fig. 17. Reaction force vs. displacement of the structure based on analytical, numerical and experimental results for low-velocity impact load.

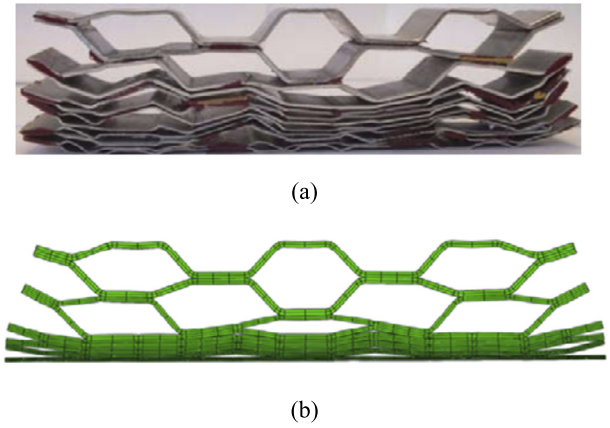

(a)

(b)

Fig. 18. Deformed shape of GHS under low-velocity impact load; (a) experimental test, (b) numerical simulation.

static loading, hence the rows may have simultaneous deformation. On the other hand, the amounts of total deformation in both cases are nearly the same. Hence, the obtained load in quasi-static case is not only related to the same row but to the last undeformed rows, as well. Fig. 14 shows the required forces are more than the analytical predicted ones and the most difference happens in the latest row. However, the difference becomes less in Fig. 17 because of different deformation mechanism as aforementioned.

According to Figs. 14 and 17, six collapse mechanisms have occurred in the model deformation. Since the model consists of six rows. In these figures, each jump and reaching to a constant force is onset of a collapse. For both quasi-static and low velocity test, six jumps are seen in Fig. 1. The first jump is for the sixth row, the second one is for fifth row and similarly the sixth one is for the first row.

It is noteworthy that the strain rate has not been considered in extracting the equation of plateau stress. Since the obtained force value for quasi-static and impact test with low velocity from experimental results is highly similar to that of analytical method, it could be concluded that the strain rate does not influence the test results in low velocity test. The strain rate has also been neglected in numerical simulation of low velocity test. Regarding the congruence between the results of numerical and experimental tests, the ineffective status of strain rate in this test has been evaluated again. Hence, the obtained analytical equations can be used for both low velocity and quasi-static loading.

In order to analyze the deformation mode of the structure under impact load with low velocity, the deformed shape of the structure acquired from experimental test and numerical simulation in different times has been demonstrated in Fig. 19.

According to Fig. 19, the mode of structure deformation in impact test with low velocity is “V” type. It is seen that the structure deformed shaped obtained from numerical simulation is properly similar to that of experimental test. Using the introduced honeycomb structure, the analytical equations and optimization algorithm the energy absorption can be increased. This kind of energy absorber can be used for elevators, infant car seat and helicopter seat for improving the crashworthiness in emergency condition.

6. Conclusion

In this research, an equation for calculating the plateau stress of a honeycomb structure has been represented based on a material model with power hardening. Moreover, the behavior of honeycomb structures under quasi-static and impact load with low velocity has been simulated in ABAQUS/CAE software. To validate the numerical simulation method and represented analytical equations, a quasi-static and impact experimental test with low velocity has been conducted. The obtained results showed that the numerical and analytical results retain an appropriate accordance with experimental results that means that the numerical simulation method and the represented analytical results are practical. Hence, the represented analytical equation can be applied to calculate the plateau stress of each row in honeycomb structure. Due to the increasing application of honeycomb structures in automotive and aeronautic science, and the costly status of manufacturing these structures for experimental tests, the represented simulation method can be utilized for studying the behavior of honeycomb structures under quasi-static and impact loading with low velocity, and for analyzing the deformation mode of this structure.

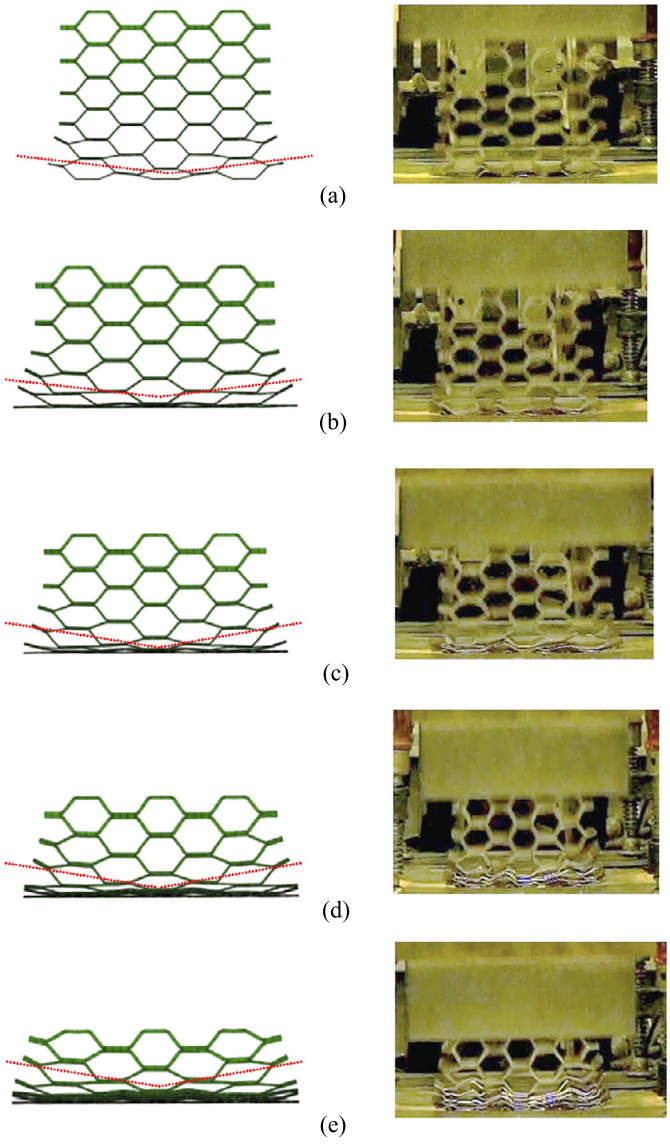

Fig. 19. Deformed shape of GHS under low-velocity impact load at different times; (a) $t = 0.375$ ms, (b) $t = 1.1$ ms, (c) $t = 1.3$ ms, (d) $t = 1.8$ ms, (e) $t = 2.4$ ms.

Conflict of interest statement

None declared.

References

[1] S. Abrate, Impact on laminated composite materials, Appl. Mech. Rev. 44 (4) (1991) 155–190.

[2] S. Adibnazari, H. Mehrabi, Effect of cell size change on honeycomb structure equivalent mechanical property, in: 10th Iran Aerospace Conference, AERO2011, Tarbiat Modarres University, 2011.

[3] A. Ajdari, H. Nayeb-Hashemi, A. Vaziri, Dynamic crushing and energy absorption of regular, irregular and functionally graded cellular structures, Int. J. Solids Struct. 48 (2011) 506–516.

[4] W.J. Cantwell, J. Morton, The impact resistance of composite materials – a review, Composites 22 (1991) 347–362.

[5] S. Deqiang, Z. Weihong, W. Yanbin, Mean out-of-plane dynamic plateau stresses of hexagonal honeycomb cores under impact loadings, Compos. Struct. 92 (2010) 2609–2621.

[6] K.P. Dharmasena, D.T. Queheillalt, H.N.G. Wadley, Y. Chen, P. Dudt, D. Knight, Z. Wei, A. Evans, Dynamic response of a multilayer prismatic structure to impulsive loads incident from water, Int. J. Impact Eng. 36 (2009) 632–643.

[7] T. Fan, G. Zou, Influences of defects on dynamic crushing properties of functionally graded honeycomb structures, J. Sandw. Struct. Mater. 17 (2015) 295–307.

[8] S.A. Galehdari, M. Kadkhodayan, Study of graded honeycomb structure under in-plane and out of plane impact loading, in: 23rd Annual International Mechanical Engineering Conference, ISME 2015, Mechanical Engineering Department, Amirkabir University of Technology, Tehran, Iran, 2015.

[9] S.A. Galehdari, M. Kadkhodayan, S. Hadidi-moud, Analytical, experimental and numerical study of a graded honeycomb structure under in-plane impact load with low velocity, Int. J. Crashworthiness 20 (2015) 387–400.

[10] M. Ghalami-Choobar, M. Sadighi, Investigation of high velocity impact of cylindrical projectile on sandwich panels with fiber–metal laminates skins and polyurethane core, Aerosp. Sci. Technol. 32 (2014) 142–152.

[11] L.J. Gibson, M.F. Ashby, Cellular Solids; Structures and Properties, 2nd edition, Cambridge University Press, 1997.

[12] R. Gunes, A. Kemal, M. Kemal, J.N. Reddy, Numerical investigations on the ballistic performance of honeycomb sandwich structures reinforced by functionally graded plates, in: 13th International Symposium on Multiscale, Multifunctional and Functionally Graded Materials, Sao Paulo, Brazil, 2014.

[13] W.Y. Jang, S. Kyriakides, On the crushing aluminum open-cell foams: Part I, experiments, Int. J. Solids Struct. 46 (2009) 617–634.

[14] A.S. Khan, S. Huang, Continuum Theory of Plasticity, John Wiley, 1995.

[15] M. Kojic, K.J. Bathe, Inelastic Analysis of Solids and Structures, Springer, 2005.

[16] Y. Liang, A.V. Spuskanyuk, S.E. Flores, D.R. Hayhurst, J.W. Hutchinson, R.M. McMeeking, A.G. Evans, The response of metal sandwich panels to water blasts, J. Appl. Mech. 74 (2007) 81–99.

[17] D. Liu, L.E. Malvern, Matrix cracking in impacted glass/epoxy plates, J. Compos. Mater. 21 (1987) 594–609.

[18] G. Lu, T.X. Yu, Energy Absorption of Structures and Materials, Wood Head Publishing Limited & CRC Press, 2003.

[19] K.R. Mangipudi, S.W. Van Buuren, P.R. Onck, The microstructural origin of strain hardening in two-dimensional open-cell metal foams, Int. J. Solids Struct. 47 (2010) 2081–2096.

[20] D. Mohr, Z. Xue, A. Vaziri, Quasi-static punch indentation of a honeycomb sandwich plate: experiments and constitutive modeling, J. Mech. Mater. Struct. 1 (2006) 581–604.

[21] L. Mori, S. Lee, Z. Xue, A. Vaziri, D.T. Queheillalt, H.N.G. Wadley, J.W. Hutchinson, H.D. Espinosa, On the behavior of sandwich structures subjected to under water impulsive loads, J. Mech. Mater. Struct. 2 (2007) 1981–2006.

[22] A. Muhammad, Study of a compact energy absorber, Ph.D. thesis, Iowa State University, 2007.

[23] A. Muhammad, J. Hoffman, J. Clark, S. Takak, Modeling of impact response of composite graded structure, in: IMECE2011, Denver, Colorado, USA, 2011.

[24] A. Muhammad, I.K. Sun, T. Matthews, Modeling of a compact functionally graded cellular structure: a finite element study for medium and high strain rates, Int. J. Mech. Mater. Des. 10 (2014) 79–92.

[25] A. Niknejad, G. Liaghat, Experimental study of Poly-orthan foam filler on hexagonal honeycomb structure behavior under axial load with constant rate, in: 10th Iran Aerospace Conference, AERO2011, Tarbiat Modarres University, 2011.

[26] S.D. Papka, S. Kyriakides, In-plane compressive response and crushing of honeycomb, J. Mech. Phys. Solids 42 (1994) 1499–1532.

[27] S.D. Papka, S. Kyriakides, In-plane crushing of a polycarbonate honeycomb, Int. J. Solids Struct. 35 (1998) 239–267.

[28] W. Prager, P.G. Hodge, Theory of Perfectly Plastic Solids, John Wiley, 1951.

[29] P. Robinson, G.A.O. Davies, Impactor mass and specimen geometry effects in low-velocity impact of laminated composites, Int. J. Impact Eng. 12 (2) (1992) 189–207.

[30] P.O. Sjoblom, J.T. Hartness, T.M. Cordell, On low-velocity impact testing of composite materials, J. Compos. Mater. 22 (1998) 30–52.

[31] Y. Song, Z. Wang, L. Zhao, J. Luo, Dynamic crushing behavior of 3D closed-cell foams based on Voronoi random model, Mater. Des. 31 (2010) 4281–4289.

[32] A. Vaziri, J.W. Hutchinson, Metal sandwich plates subject to intense air shocks, Int. J. Solids Struct. 44 (2007) 2021–2035.

[33] J. Xiong, L. Ma, L. Wu, M. Li, A. Vaziri, Mechanical behavior of sandwich panels with hollow Al–Si alloy tubes core construction, Mater. Des. 32 (2011) 592–597.

[34] T.X. Yu, L.C. Zhang, Plastic Bending: Theory and Applications, Series of Engineering Mechanics, vol. 2, World Scientific Pub. Co. Inc., 1996.

[35] H.X. Zhu, Large deformation pure bending of an elastic plastic power-law-hardening wide plate: analysis and application, Int. J. Mech. Sci. 49 (2007) 500–514.

[36] Z. Zou, S.R. Reid, P.J. Tan, S. Li, J.J. Harrigan, Dynamic crushing of honeycombs and features of shock fronts, Int. J. Impact Eng. 36 (2009) 165–167.